BJC OPEN

Effect of PI3K- and mTOR-specific inhibitors on spontaneous B-cell follicular lymphomas in PTEN/LKB1-deficient mice

JM García-Martínez[1,6], S Wullschleger[1,6], G Preston[2], S Guichard[3], S Fleming[4], DR Alessi*,[1] and SL Duce*,[5]

[1]MRC Protein Phosphorylation Unit, College of Life Sciences, University of Dundee, Dundee DD1 5EH, UK; [2]Division of Cell Biology and Immunology, College of Life Sciences, University of Dundee, Dundee DD1 5EH, UK; [3]Cancer Bioscience, AstraZeneca, Alderley Park, Cheshire SK10 4TG, UK; [4]Department of Molecular Pathology, University of Dundee, Ninewells Hospital, Dundee DD1 9SY, UK; [5]Division of Biological Chemistry and Drug Discovery, College of Life Sciences, University of Dundee, Dundee DD1 5EH, UK

BACKGROUND: The PI3K–mTOR (phosphoinositide 3-kinase–mammalian target of rapamycin kinase) pathway is activated in the majority of tumours, and there is interest in assessing whether inhibitors of PI3K or mTOR kinase have efficacy in treating cancer. Here, we define the effectiveness of specific mTOR (AZD8055) and PI3K (GDC-0941) inhibitors, currently in clinical trials, in treating spontaneous B-cell follicular lymphoma that develops in PTEN$^{+/-}$LKB1$^{+/hypo}$ mice.

METHODS: The PTEN$^{+/-}$LKB1$^{+/hypo}$ mice were administered AZD8055 or GDC-0941, and the volumes of B-cell follicular lymphoma were measured by MRI. Tumour samples were analysed by immunohistochemistry, immunoblot and flow cytometry.

RESULTS: The AZD8055 or GDC-0941 induced ~40% reduction in tumour volume within 2 weeks, accompanied by ablation of phosphorylation of AKT, S6K and SGK (serum and glucocorticoid protein kinase) protein kinases. The drugs reduced tumour cell proliferation, promoted apoptosis and suppressed centroblast population. The AZD8055 or GDC-0941 treatment beyond 3 weeks caused a moderate additional decrease in tumour volume, reaching ~50% of the initial volume after 6 weeks of treatment. Tumours grew back at an increased rate and displayed similar high grade and diffuse morphology as the control untreated tumours upon cessation of drug treatment.

CONCLUSION: These results define the effects that newly designed and specific mTOR and PI3K inhibitors have on a spontaneous tumour model, which may be more representative than xenograft models frequently employed to assess effectiveness of kinase inhibitors. Our data suggest that mTOR and PI3K inhibitors would benefit treatment of cancers in which the PI3K pathway is inappropriately activated; however, when administered alone, may not cause complete regression of such tumours.

Translational Therapeutics

The majority of human cancers possess mutations in signal transduction components that lead to the over-activation of phosphoinositide 3-kinase (PI3K) and mammalian target of rapamycin kinase (mTOR) signalling pathways. The PI3K is activated downstream of growth factor receptors and phosphorylates phosphatidyl 4,5-bisphosphate (PtdIns(4,5)P$_2$) to produce the PtdIns(3,4,5)P$_3$ second messenger. This promotes the activation of the 3-phosphoinositide-dependent protein kinase-1 (PDK1) as well as the two mTOR multiprotein complexes, mTOR complex-1 (mTORC1; including mTOR, Raptor and mLST8) and mTOR complex-2 (mTORC2; including mTOR, Rictor, Sin1, mLST8 and Protor), which will lead in turn to the activation of downstream kinases including isoforms of Akt, p70 ribosomal S6 kinase (S6K) and the serum and glucocorticoid protein kinase (SGK) (Pearce et al, 2010). Activation of this signalling network has vital roles in promoting growth, survival and proliferation of cancer cells

(Engelman et al, 2006). The importance of this network in cancer is emphasised by the finding that many cancer-driving mutations stimulate this pathway. These include activating mutations of the catalytic subunit of PI3K-α (Samuels et al, 2004) or mutations that inactivate the lipid phosphatase and tensin homologue deleted on chromosome 10 (PTEN) that degrades PtdIns(3,4,5)P$_3$ (Sulis and Parsons, 2003; Leslie and Downes, 2004). Consistent with this, heterozygous PTEN$^{+/-}$ mice spontaneously develop a variety of tumours after 8 months of age (Di Cristofano et al, 1998; Haas-Kogan et al, 1998; Maehama and Dixon, 1998; Myers et al, 1998; Stambolic et al, 1998; Suzuki et al, 1998; Podsypanina et al, 1999), and importantly, tumour development in PTEN-deficient mice is significantly suppressed by genetic disruption of PDK1 (Bayascas et al, 2005; Wullschleger et al, 2010), mTOR complex components (Guertin et al, 2009) or Akt (Chen et al, 2006).

These observations have led to huge efforts to develop inhibitors that suppress the PI3K and mTOR pathways that are beginning to be evaluated in clinical trials (Engelman, 2009). Two such compounds are GDC-0941, a PI3K inhibitor (Folkes et al, 2008; Salphati et al, 2010), and AZD8055, an mTOR inhibitor (Chresta et al, 2010). The GDC-0941 inhibits all class 1 PI3K isoforms (IC50 of 3 nM PI3K-α, 33 nM PI3K-β, 3 nM PI3K-δ and 75 nM PI3K-γ) but does not significantly suppress the activity of any other lipid or

---

*Correspondence: Professor DR Alessi or Dr SL Duce;
E-mails: d.r.alessi@dundee.ac.uk or s.duce@dundee.ac.uk
[6]These authors contributed equally to this work.

protein kinase tested including mTOR (Folkes *et al*, 2008). The AZD8055 is also a remarkably potent mTOR kinase inhibitor (IC50 of 0.13 nM), suppressing activity of both mTORC1 and mTORC2 without inhibiting PI3K isoforms or any other lipid or protein kinases tested (Chresta *et al*, 2010). Recent pharmacokinetic–pharmacodynamic data indicate that GDC-0941 (Salphati *et al*, 2010) and AZD8055 (Chresta *et al*, 2010) are well tolerated and effective in mice, and these studies have also shown that GDC-0941 and AZD8055 slow the growth of several cancer cells that have elevated PI3K pathway activity in xenografts mice models.

In this study, we evaluated the effects that administration of GDC-0941 or AZD8055 had on spontaneous B-cell follicular lymphomas developed in 6- to 8-month-old heterozygous $PTEN^{+/-}LKB1^{+/hypo}$ mice. Our data suggests that, at least for this type of tumour driven by activation of the PI3K and mTOR pathway, single-agent administration of drugs that suppress these pathways would be effective at shrinking tumours and inhibiting their growth, but would not cause complete regression.

MATERIALS AND METHODS

Materials

Protein G-Sepharose was purchased from Amersham Bioscience (Uppsala, Sweden); $^{32}P\gamma$-ATP was from Perkin-Elmer (Boston, MA, USA); Tween-20 and DMSO were from Sigma (Steinheim, Germany); and CHAPS was from Calbiochem (La Jolla, CA, USA). The GDC-0941 was synthesised by Dr Natalia Shpiro at the University of Dundee. The AZD8055 was provided by AstraZeneca (Alderley Park, Cheshire, UK). For studies in mice, both drugs were dissolved in a final captisol (CyDex, Lenexa, KS, USA) concentration of 30% (w/v). The GDC-0941 ($75\,mg\,kg^{-1}$) and AZD8055 ($20\,mg\,kg^{-1}$) were administered by oral gavage once daily for up to 42 days.

Mice breeding, genotyping and tumour analysis

All animal studies were approved by the University of Dundee Ethics Committee and performed under a UK Home Office project license. The generation and genotyping of the $PTEN^{+/-}$ mice (Podsypanina *et al*, 1999) the LKB1 hypomorphic mice (Sakamoto *et al*, 2005) have been described previously. The parental $LKB1^{+/hypo}$ and $PTEN^{+/-}$ used for these experiments had been backcrossed with C57BL/6J for over seven generations before initiating the crosses for the present study. Littermates with different genotypes of LKB1 and PTEN were generated and maintained under standard husbandry conditions for a period of up to 14 months of age. During this period, mouse weight and blood glucose levels were routinely monitored. Onset of tumour formation was monitored by weekly palpation of the major lymph nodes. According to our UK Home Office license, any animal that displayed an obvious external tumour of over $1.44\,cm^2$ or showed signs of sickness was culled. The tissues were fixed in 10% formalin and subjected to necropsy and pathological analysis. Tumour slices were generated and analysed as described previously (Bayascas *et al*, 2005).

Magnetic resonance imaging

Mice were anesthetised with 1.5% isoflurane in 100% oxygen using a nose cone with scavenging. The mice were monitored during imaging and recovery, and then returned to their cage. The MRI data were acquired on a Bruker Avance FT NMR spectrometer (Bruker Biospin GmbH, Rheinstetten, Germany) with a wide-bore 7.1-Tesla vertical magnet (Oxford Instruments, Abingdon, Oxfordshire, UK) resonating at 300.15 MHz for ^{1}H. A MicroMouse birdcage radio-frequency resonator (Bruker Biospin GmbH, Rheinstetten, Germany) with an internal diameter of 30 mm was used. Three-dimensional (3D) 128 by 128 by 128 rapid acquisition relaxation enhanced (RARE) MRI experiments were performed

with RARE factor of 4, taken from the Paravision library (Bruker Biospin GmbH). Recycle time (TR) of 250 ms and an effective echo time (TE) of 10 ms were used. One acquisition sequence was acquired to minimise experimental time, which was 16 min. The field of view was 30 mm and isotropic image spatial resolution was $234\,\mu m$ per pixel.

MRI data analysis

The MRI data were Fourier transformed and then visualised using Amira PC-based software (Visage Imaging GmbH, 12163 Berlin, Germany). This allowed 2D slices to be viewed from any angle within the 3D data set and allowed digital segmentation. The anatomy of interest was digitally segmented, 3D finite element meshes generated and surface rendered to produce 3D surface representations. This allowed the volumes of the tumours to be calculated.

Buffers

The following buffers were used: Tris lysis buffer (50 mM Tris-HCl (pH 7.5), 1 mM EGTA, 1 mM EDTA, 0.3 % (w/v) CHAPS, 1 mM sodium orthovanadate, 10 mM sodium-β-glycerophosphate, 50 mM sodium fluoride, 5 mM sodium pyrophosphate, 0.27 M sucrose, 0.15 M NaCl, 0.1 % (v/v) 2-mercaptoethanol, 1 mM benzamidine and 0.1 mM phenylmethylsulphonylfluoride); Buffer A (50 mM Tris-HCl (pH 7.5), 0.1 mM EGTA and 0.1% (v/v) 2-mercaptoethanol); TBS-Tween buffer (50 mM Tris-HCl (pH 7.5), 0.15 M NaCl and 0.1% (v/v) Tween-20); and Sample buffer (50 mM Tris-HCl (pH 6.8), 6.5% (v/v) glycerol, 1% (w/v) SDS and 1 % (v/v) 2-mercaptoethanol).

Preparation of tissue lysates

Tissues were extracted, frozen in liquid nitrogen and stored at $-80°C$. Tissues were homogenised on ice in a 10-fold mass excess of ice-cold Tris lysis buffer using a Kinematica Polytron (Kinematica, Littan, Switzerland). Tissue lysates were centrifuged at 18 000 *g* for 15 min at 4°C, and the supernatant was snap frozen in aliquots and stored at $-80°C$.

Kinase assays

Tumours were lysed in Tris lysis buffer. To perform Akt and S6K assays, $500\,\mu g$ of lysate was incubated with $1-5\,\mu g$ of the corresponding antibody conjugated to protein G-sepharose. All the incubations were performed for 1 h at 4°C on a vibrating platform. Kinase activity was assayed using the crosstide peptide (GRPRTSSFAEG) at $30\,\mu M$. Incorporation of [^{32}P]-phosphate into the peptide substrate was determined by applying the reaction mixture on to P81 phosphocellulose paper, and scintillation counting after washing the papers in phosphoric acid. One unit of activity was defined as that amount of enzyme that catalysed the incorporation of 1 nmol of [^{32}P]-phosphate into the substrate.

Immunoblotting

Total tumour lysate ($5-20\,\mu g$) was heated at 95°C for 5 min in sample buffer, and subjected to polyacrylamide gel electrophoresis and electrotransfered to nitrocellulose membrane. Membranes were blocked for 1 h in TBS-Tween buffer containing 10% (w/v) skimmed milk. The membranes were probed with the indicated antibodies in TBS-Tween containing 5% (w/v) skimmed milk or 5% (w/v) BSA for 16 h at 4°C. Detection was performed using horseradish peroxidase-conjugated secondary antibodies and the enhanced chemiluminescence reagent.

Antibodies

The following antibodies were raised in sheep and affinity purified on the appropriate antigen: anti-NDRG1 (S276B, second bleed) was made in sheep using recombinant GST fusion of full-length

NDRG1 (used for immunoblotting). An antibody that recognises NDRG1 phosphorylated at Thr346, Thr356 and Thr366 (S911B, second bleed; termed pNDRG1 3xThr-P) was raised against the nonapeptide RSRSHpTSEG, whose sequence is common to all three SGK1 phosphorylation sites on NDGR1 (used for immunoblotting). Anti-Akt1 (S742B, third bleed) was made in sheep using recombinant His-Akt1 (used for immunoblotting and immunoprecipitation), anti-S6K (S417B, second bleed; residues 25–44 of human S6K AGVFDIDLDQPEDAGSEDEL, used for immunoblotting and immunoprecipitation). Anti-PRAS40 (S115B, first bleed; residues 238–256 of human PRAS40 DLPRPRLNTSDFQKLKRKY, used for immunoblotting). An antibody that recognises PRAS40 phosphorylated at Thr246 (S114B, second bleed) was raised against the residues 240–251 of human PRAS40 CRPRLNTpSDFQK (used for immunoblotting). Anti-FoxO1 (S504A, last bleed) was made in sheep using recombinant GST-fusion FoxO1 (2-655, used for immunoblotting). The phospho-Akt Ser473 (no. 9271), Thr308 (no. 4056), phospho-S6K Thr389 no. 9234), phospho-S6 ribosomal protein Ser235 (no. 4856), total S6 ribosomal protein (no. 2217), phospho-FoxO1/O3 Thr24/32 (no. 9464), phospho-GSK3α/β Ser21/9 (no. 9331), phospho-4E-BP1 Thr37/Thr46 (no. 9459), phospho-4E-BP1 Thr65 (no. 9451), phospho-4E-BP1 Ser70 (no. 9455) and total 4E-BP1 (no. 9452) were purchased from Cell Signaling Technology (Danvers, MA, USA). For phosphor immunoblotting of the phosphorylated T-loop of S6K, we employed the pan-PDK1-site antibody from Cell Signaling Technology no. 9379) as previously described (Collins *et al*, 2005). The GSK3α/β antibody (44-610) was purchased from Biosource (Camarillo, CA, USA). The secondary antibodies coupled to horseradish peroxidase used for immunoblotting were obtained from Thermo Scientific (Rockford, IL, USA).

IHC staining

Primary antibodies were used to detect B220/CD45R (RA3-6B2, BD Pharmingen, Oxford Science Park, Oxford, UK), CD79αcy (HM57, Dako, Ely, Cambridgeshire, UK), CD3 (F7.2.38, Dako) and Ki67 (VP-K452, Vector Laboratories, Peterborough, UK). Antibodies against Akt p-473 (no. 9277), caspase-3 (no. 9662) and S6 p-S235/S236 (no. 4857) were purchased from Cell Signaling Technology. Antibody binding was visualised using Vectastain reagents (Vector Laboratories) and protocols performed on a Dako immunostainer. Sections were viewed on a Nikon Eclipse E600 microscope, and digital images captured on a Nikon DXM 1200 digital camera (Nikon UK, Kingston Upon Thames, Surrey, UK).

Flow cytometric analysis

Cells were extracted from tumour and control lymph node samples by mashing through 70 μM filters into media (RPMI 1640 supplemented with 10% fetal calf serum, 100 IU ml^{-1} penicillin, 100 μg ml^{-1} streptomycin and 50 μM β-mercaptoethanol). Cells were then counted and 5×10^5 cells were taken per point for staining. The following antibodies were used for staining the samples: TCRβ-APC, B220-PE, CD4-FITC, κ-light-chain-PE, λ-light-chain-FITC, B220-APC (BD Pharmingen) and CD8-PECy5.5 (Invitrogen, Camarillo, CA, USA). Live cells were identified by forward–side scatter profile. B cells were identified by B220 expression and T cells by TCRβ expression. The κ- and λ-ratios were calculated on B220-positive cells.

RESULTS

The AZD8055 and GDC-0941 oral administrations inhibit S6K, AKT and SGK activity within the tumours

We employed previously described PTEN$^{+/-}$LKB1$^{+/\text{hypo}}$ mice that are heterozygous for the expression of PTEN and express 60% of the normal levels of LKB1 in all tissues studied (Huang *et al*,

2008). Approximately 90% of these mice develop spontaneously large B-cell follicular lymphomas within cervical lymph nodes between 6 and 8 months of age (Huang *et al*, 2008). To investigate whether it was feasible to effectively inhibit the PI3K–mTOR pathway within tumours, we treated PTEN$^{+/-}$LKB1$^{+/\text{hypo}}$ mice bearing visible tumours with either vehicle alone, AZD8055 (20 mg kg^{-1}) or GDC-0941 (75 mg kg^{-1}) once daily for 5 days. The kinase inhibitors were well tolerated, and no changes on overall mouse weight or health were detected during the treatment. As previously described (Chresta *et al*, 2010), we observed that GDC-0941 or AZD8055 administration induced a transient increase in blood glucose levels (Supplementary Figure 1). This is consistent with these compounds suppressing the PI3K–mTOR pathway and thereby inhibiting insulin signalling and leading to transient insulin resistance. After 5 days of treatment, tumours were dissected and protein extracts generated. In tumour extracts derived from PTEN$^{+/-}$LKB1$^{+/\text{hypo}}$ mice not administered with kinase inhibitors, a high level of Akt kinase activity and phosphorylation of Thr308 (PDK1 site) and Ser473 (mTORC2 site) were observed (Figure 1A, chart and upper panel). As expected, treatment with either AZD8055 or GDC-0941 led to a marked inhibition of Akt activity as well as phosphorylation of Thr308 and Ser473 (Figure 1A, chart and upper panel). Phosphorylation of the Akt substrates PRAS40 and Foxo-1/3a were also inhibited by AZD8055 or GDC-941, but phosphorylation of GSK3α/GSK3β, which can be regulated by multiple kinases (RSK, PKC and PKA), was hardly affected (Figure 1A, lower panel). Inhibition of Thr308 phosphorylation was slightly more pronounced after GDC-0941 administration than observed with AZD8055, and similar effect was observed in Foxo-1/3a phosphorylation (Figure 1A).

We also observed significant S6K1 activity and phosphorylation at Thr229 (PDK1 site) and Thr389 (mTORC1 site) in tumour extracts derived from non-drug-treated PTEN$^{+/-}$LKB1$^{+/\text{hypo}}$ animals (Figure 1B, chart and upper panel). The AZD8055 or GDC-0941 treatment almost ablated S6K1 activity and suppressed phosphorylation of Thr229 and Thr389 (Figure 1B, upper panel). Both drugs also inhibited phosphorylation of the ribosomal S6 protein, an S6K substrate (Figure 1B, lower panel). We also investigated the effects that these drugs had on 4E-BP1, a key regulator of protein synthesis whose phosphorylation is induced by the mTOR pathway (Wullschleger *et al*, 2006). We found that AZD8055 and GDC-0941, to a lesser extent, induced a marked increase in the electrophoretic mobility of 4E-BP1 within tumour samples, which was accompanied by marked dephosphorylation of Thr37/Thr46 and Ser65 (Figure 1C). AZD8055 or GDC-0941 did not induce dephosphorylation of Thr70 on 4E-BP1, suggesting this residue is not regulated by the PI 3-kinase or mTOR pathway, which is consistent with previous work (Thoreen *et al*, 2009).

Currently, it is not possible to reliably assay the activity of endogenous SGK isoforms because of lack of antibodies; hence, we instead examined the phosphorylation of the SGK1 N-myc downstream-regulated gene-1 (NDRG1) substrate, as readout for SGK1 activity (Murray *et al*, 2004; Garcia-Martinez and Alessi, 2008). This revealed that AZD8055 or GDC-0941 also markedly inhibited phosphorylation of endogenous NDRG1 at the site phosphorylated by SGK1 in tumour extracts (Figure 1D).

The mTOR and PI3K inhibition impairs tumour growth and development

We next attempted to establish how AZD8055 or GDC-0941 administration affected the progression of spontaneous B-cell cervical follicular lymphomas in PTEN$^{+/-}$LKB1$^{+/\text{hypo}}$ animals. We used 6- to 8-month-old PTEN$^{+/-}$LKB1$^{+/\text{hypo}}$ mice that had developed externally visible tumours. At this stage, the volume of tumours was measured by MRI, tumours were visible in the 2D image and appeared darker than the neighbouring submaxillary and sublingual salivary glands, whereas subcutaneous adipose

BJC
OPEN

PI3K and mTOR inhibitors shrink follicular lymphomas
JM García-Martínez et al

npg

1119
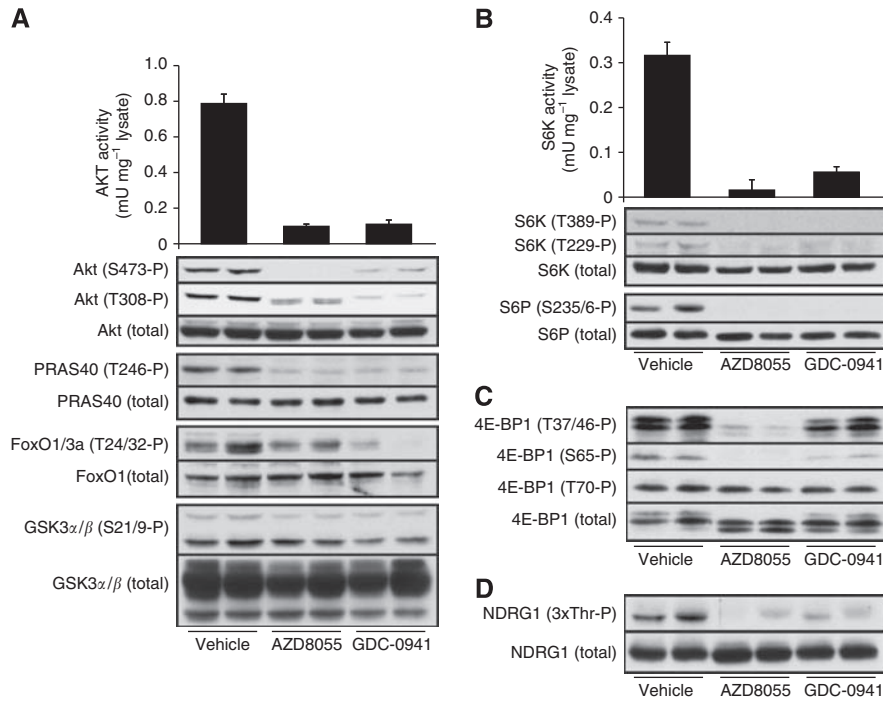
Figure 1 The AZD8055 and GDC-0941 oral administration suppresses PI3K downstream signalling within the tumours. The PTEN$^{+/-}$LKB1$^{+/hypo}$ mice bearing visible tumours were treated with either vehicle, AZD8055 (20 mg kg^{-1}) or GDC-0941 (75 mg kg^{-1}) once daily by oral gavage for 5 days. At 2 h after the final dose, mice were culled and tumour samples were generated. (**A**) The AKT was immunoprecipitated from tumour lysates, and catalytic activity assessed employing the crosstide substrate. Each bar represents the mean specific activity ± s.e. from three to five different samples, with each sample assayed in duplicate. Tumour lysates were also analysed by immunoblotting with the indicated antibodies. (**B**) As in (**A**), except that S6K was immunoprecipitated and its catalytic activity assessed. (**C**) Tumour extracts were immunoblotted with the indicated phospho and total 4E-BP1 antibodies. (**D**) SGK1 activity was assessed only by phosphorylation of the SGK1-substrate NDRG1. For each condition, immunoblots are shown with duplicate samples derived from different mice.
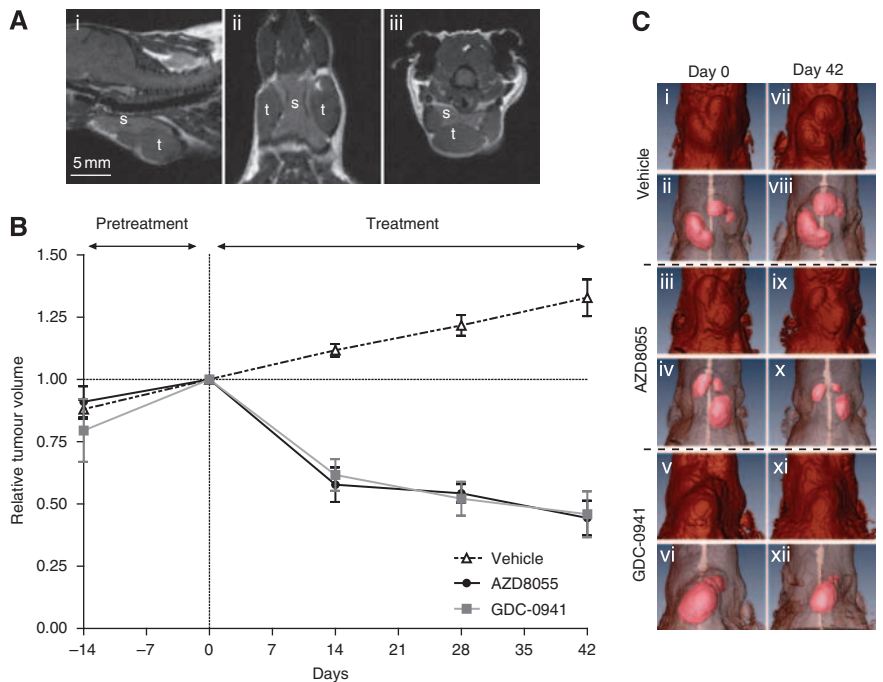
Figure 2 Tumour regression induced by AZD8055 and GDC-0941 oral administration. (**A**) The 2D MRI images from 3D RARE-4 MRI data set of the neck of heterozygous PTEN$^{+/-}$LKB1$^{+/hypo}$ mouse before treatment; (i) sagittal image, (ii) ventral transverse image and (iii) anterior frontal image, highlighting tumours (t) and submaxillary salivary gland(s). (**B**) Mean relative tumour volumes (normalised to their size at day 0) plotted against time. Dashed line (triangles) indicates mice treated with vehicle alone (n = 5), black line (circles) indicates mice treated with AZD8055 (20 mg kg^{-1}; n = 5) and grey line (squares) represents GDC-0941 (75 mg kg^{-1}; n = 4) treatment. (**C**) Ventral transverse views of 3D surface reconstructions of MRI from the neck region of three heterozygous PTEN$^{+/-}$LKB1$^{+/hypo}$ mice acquired first at day 0 (before treatment; i–vi), and again at day 42 (end of treatment; vii–xii). The skin is shown in brown, tumours in pink and trachea in white.

Translational Therapeutics

PI3K and mTOR inhibitors shrink follicular lymphomas
JM García-Martínez et al

npg

BJC
OPEN

1120

tissue was white. Other anatomical features, such as the trachea and blood vessels, were visible and appeared black (Figure 2A). Tumour volumes in the mice was reassessed by MRI after 2 further weeks without drug treatment, where an increase in volume by $\sim 15\%$ was found (Figure 2B). The mice were then administered daily doses of vehicle alone, AZD8055 ($20 \, mg \, kg^{-1}$) or GDC-0941 ($75 \, mg \, kg^{-1}$) for 42 days by oral gavage, and tumour volume was monitored every 2 weeks (Figure 2B). Inhibitor treatment was well tolerated, and there was no change on overall health status of the animals at any time point analysed. Total volume of the tumours for each mouse at each time point was measured and tabulated (Supplementary Table 1), and normalised by assigning the tumour volume as 1 at day 0 (before drug administration initiated). In mice treated with vehicle, tumours continued to expand approximately linearly with a mean growth rate of $11.8 \pm 9.0 \, mm^3$ per week (Figure 2B). Strikingly, in both AZD8055- and GDC-0941-treated mice, there was a marked regression of tumours from days 0 to 14, where they shrunk to $\sim 40\%$ of their original size. After 2 weeks, tumour shrinkage slowed and became more static, and by day 42, the tumours treated with either inhibitor had shrunk to about half their original size (Figure 2B). Representative tumour segmentations before treatment at day 0, and at the end of treatment at day 42, are illustrated in Figure 2C.

Effect of AZD8055 and GDC-0941 treatment on tumour morphology

To evaluate the effect of the kinase inhibitors on tumour morphology, an additional group of $PTEN^{+/-}LKB1^{+/hypo}$ mice bearing visible tumours was treated for 14 days, corresponding to the maximal tumour regression observed by MRI. Necropsy was performed, and the tissues were fixed in 10% formalin and subjected to a detailed examination by histopathological and immunocytochemical methods. As previously described for this type of tumour in $PTEN^{+/-}LKB1^{+/hypo}$ mice, the neck masses were confirmed to be B-cell lymphomas (Bayascas et al, 2005; Huang et al, 2008; Wullschleger et al, 2010). There was effacement of the lymph node architecture associated with follicular lymphoma (Figures 3A) showing immunoreactivity for B220/CD45R and CD79α, and only a minority of cases showed Bcl-2 reactivity. T cells detected by anti CD3 were found in the interfollicular areas (data not shown). The neoplastic follicles contained a mixture of large centroblast cells and a majority of small centrocytes (Figure 3B). The Ki67 reactivity was seen in 10–15% of follicular cells (Figure 3C). The centroblasts showed strong cytoplasmic staining for phosphorylated ribosomal S6 protein (Figure 3E), and diffuse cytoplasmic staining of tumour cells for Akt Ser473 phosphorylation was also detected (Figure 3F). A comparison of tumours from the control group with those from mice that had been treated for 2 weeks with either AZD8055 or GDC-0941 highlights significant changes in morphology. The lymph nodes from mice treated with AZD8055 or GDC-0941 were smaller and show a replacement by lymphoma that was follicular with a mixture of centrocytes and centroblasts (Figures 3G, H, M and N). The Ki67 reactivity fell to below 5% of the neoplastic follicular cell population (Figures 3I and O). Interestingly, there was increased apoptosis, measured by morphology and immunoreactivity for activated caspase-3 (Figures 3J and P; data not shown). Consistent with the effect of the inhibitors ablating S6K1 activity, staining for phosphorylated ribosomal S6 protein in centroblasts was diminished in comparison with controls (Figures 3K and Q). However, the diffuse cytoplasmic staining for Akt Ser473 phosphorylation was still detected by immunohistochemistry in treated lymphomas (Figures 3L and R).

In addition, tumour samples from mice in the longitudinal MRI study that been treated for 42 days were also analysed by both immunohistochemistry and immunoblot. Consistent with the 14 days data, histopathological examination of untreated animals

showed large lymph nodes with continued growth of the follicular lymphoma showing Ki67 reactivity of 15–20% (Figure 4A, panels a and b). There was a continued strong reactivity for phosphorylated ribosomal S6 protein (Figure 4A, panel c). In contrast, the tumours from animals treated with either AZD8055 or GDC-0941 had much smaller lymph nodes and a low Ki67 reactivity ($<5\%$; Figure 4A, panels d, e, g and h). Plus, the staining for phosphorylated ribosomal S6, was clearly reduced (Figure 4A, panels f and i). This demonstrates that the inhibitor treatment after 42 days was still effective in spite of the reduced regression of tumour growth. We also detected a clear inhibition of the S6K1 activity measured as phosphorylation of the ribosomal S6 protein in the immunoblot analysis (Figure 4B, upper panel). Despite the diffuse cytoplasmic staining for Akt Ser473 phosphorylation detected by immunohistochemistry in treated lymphomas, more quantitative analysis by western blot showed a clear suppression of Akt Ser473 and Thr308 phosphorylation (Figure 4B, medium panel). Phosphorylation of the Akt substrates PRAS40 and Foxo-1/3a was also inhibited, again with an enhanced effect on Foxo-1/3a phosphorylation in GDC-0941-treated tumours (Figure 4B, medium panel). As previously observed, no major effect on in GSK3α/GSK3β phosphorylation was detected after inhibitor treatment (Figure 4B, medium panel). Finally, phosphorylation of endogenous NDRG1 was also inhibited by both AZD8055 and GDC-0941 treatments in tumour lysates (Figure 4B, lower panel).

AZD8055 and GDC-0941 treatment effectively reduces B-cell centroblast population

Flow cytometric analysis was also performed in healthy lymph node samples as well as in tumour samples derived from mice treated for 42 days. The aim was to ascertain whether the shrinkage of the tumours induced by drug treatment represented a specific effect on the malignant B cells.

As expected, lymphomas showed a marked increase in the percentage of B cells compared with healthy lymph nodes (Figure 5A). Drug treatment with either AZD8055 or GDC-0941 had no obvious effect on restoring the physiological B:T cell ratio (Figure 5A). There was no difference in κ- or λ-immunoglobulin light-chain expression between tumours or control lymph nodes (Figure 5B). However, 95% of normal mature mouse B cells show usage of κ-light chains; hence, demonstration of light-chain restriction is less valuable in murine than in human lymphomas (Taddesse-Heath and Morse, 2000).

The majority of B cells found within the tumour remain small (centrocytes), but there are an increased number of large cells (centroblast) compared with control lymph nodes. A higher number of large cells within the tumour signify a higher grade of tumour and a more aggressive clinical course (Harris et al, 1999). After excluding doublets, we quantified the centroblast population of B cells within the tumours by forward/side scatter profile (Figure 5C). Intriguingly, this population was dramatically reduced by drug treatment with either AZD8055 or GDC-0941. In contrast, no significant differences were detected between treated and untreated tumour T-cell populations by forward/side scatter profile (data not shown).

Tumour re-growth following cessation of drug treatment

To study the effect that cessation of drug administration had on tumour growth, a new group of $PTEN^{+/-}LKB1^{+/hypo}$ mice bearing visible tumours was treated with either vehicle alone, AZD8055 ($20 \, mg \, kg^{-1}$) or GDC-0941($75 \, mg \, kg^{-1}$) for 42 days. Consistent with our previous results, after this treatment, tumours in drug-treated animals diminished in volume by $\sim 50\%$ (Figure 6A). At day 42, drug administration ceased, and mice were monitored for an additional 5 weeks during which tumour volume for each mouse was analysed by MRI at days 63 and 77 and the total tumour
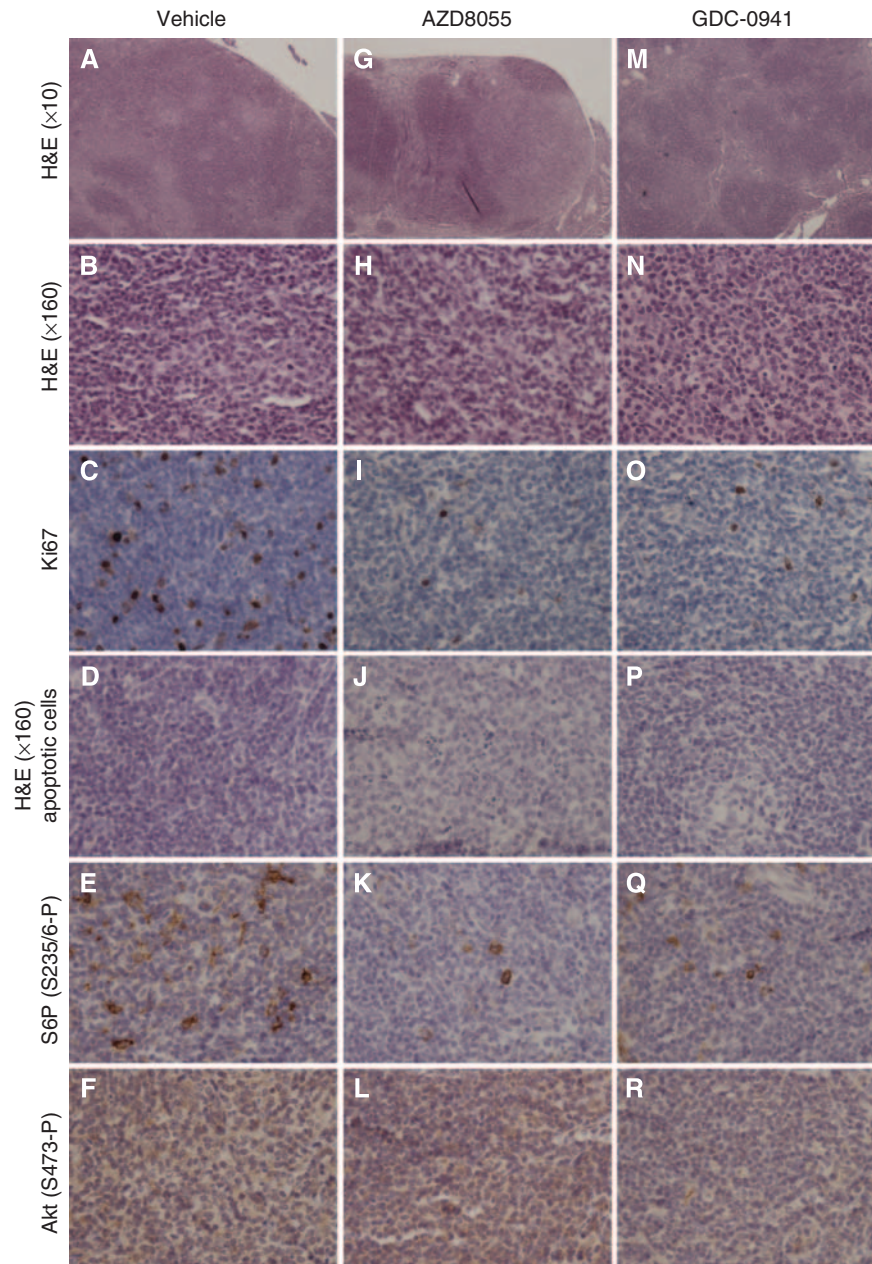
Figure 3 Tumour morphology after 14 days of drug treatment. At 2 h after the final dose (day 14), mice ($n = 3$) were culled, and tumour samples were processed for histopathological and immunocytochemical analysis. Representative sections of H&E staining ($\times 10$ and $\times 160$ objective) and immunohistochemistry of lymphomas using the indicated antibodies are shown. The lymphomas were all classified as B-cell follicular lymphoma by the Bethesda criteria. (**A–F**) represent tumour sections from vehicle treated mice, (**G–L**) are sections from AZD8055 treated mice and (**M–R**) are sections from GDC-0941 treated mice.

volume was normalised to its value at day 0 (Figure 6A). This data revealed that following the removal of drug, the tumours start growing markedly. In the case of AZD8055 treatment, tumours reached their original size before drug administration within ~ 30 days, and for GDC-0941, within ~ 16 days after cessation of treatment (Figure 6A). We also calculated the relative rates of tumour re-growth following removal of drug by normalising total tumour volume to its value at day 42 (cessation of treatment; Figure 6B). The mean growth rates of tumours from days 42 to 77 were $11.8 \pm 9.0\,\text{mm}^3$ per week (mice not treated with drug), $21.2 \pm 5.6\,\text{mm}^3$ per week (mice treated with AZD8055) and $29 \pm 6.5\,\text{mm}^3$ per week (mice treated with GDC-0941; Supplementary Table 1),

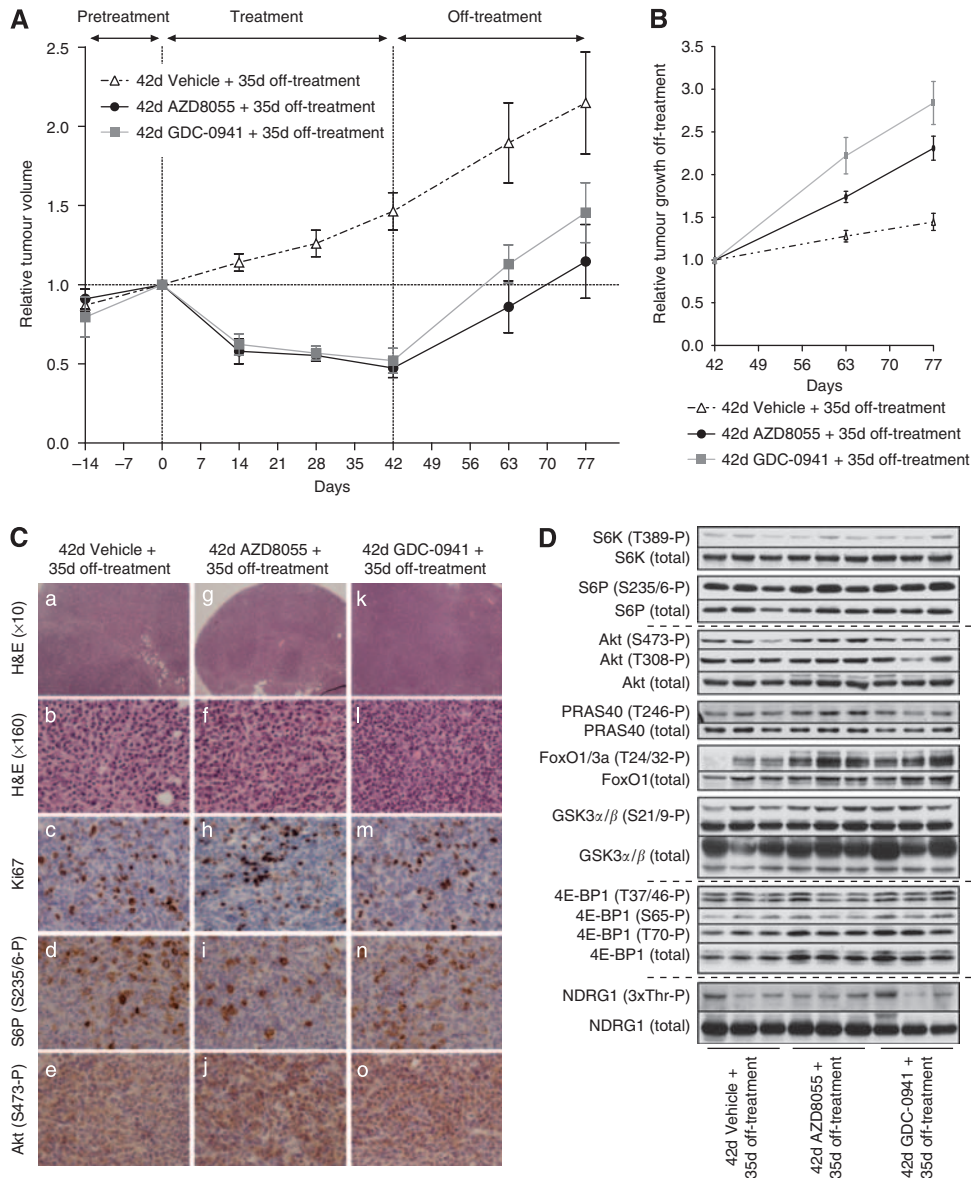indicating that the drug-treated tumours re-grew around twice the rate of the untreated tumour.

Histopathological and immunocytochemical examination of extracted tumours at day 77 showed that animals in the control group showed progression from follicular to diffuse large B-cell lymphoma, with a Ki67 rate of 15–20% and strong phosphorylated ribosomal S6 protein reactivity (Figure 6C, panels a–d). Moreover, and consistently with the tumour re-growth, following cessation of either AZD8055 or GDC-0941 for 5 weeks, the morphology of the tumours from these mice also showed a trend towards progression to diffuse large B-cell lymphoma (Figure 6C, panels g, f, k and l). Tumours in these animals also showed a markedly
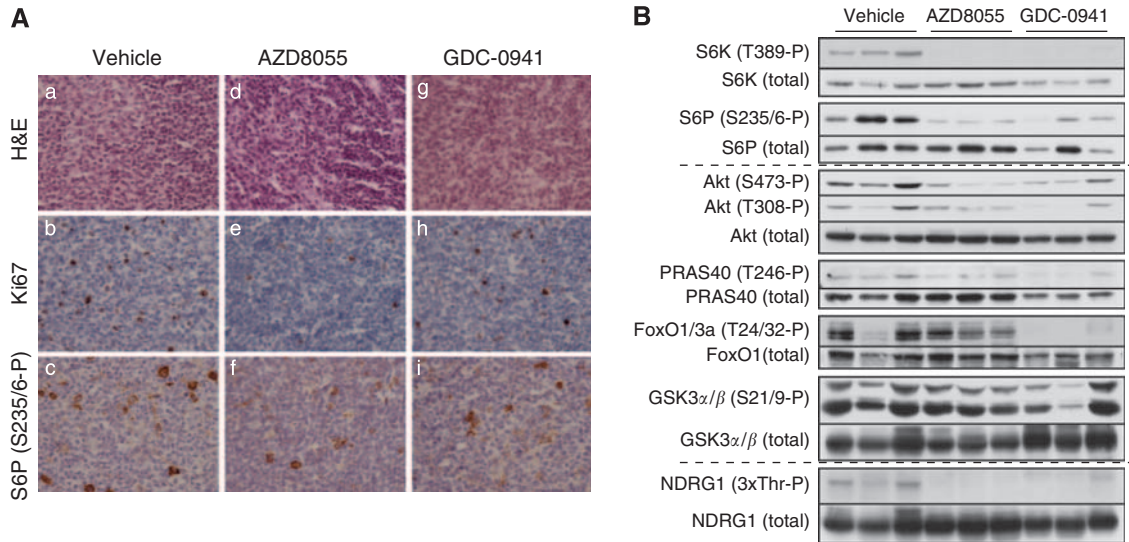
Figure 4 PI3K downstream signalling at MRI-analysis end point. As in Figure 3, tumour samples were processed for immunohistological analysis with the indicated staining (**A**); or total tumour lysates were generated and analysed by immunoblotting with the indicated antibodies (**B**). For each condition, immunoblots and immunostainings are representative tumour samples derived from four to five different mice.
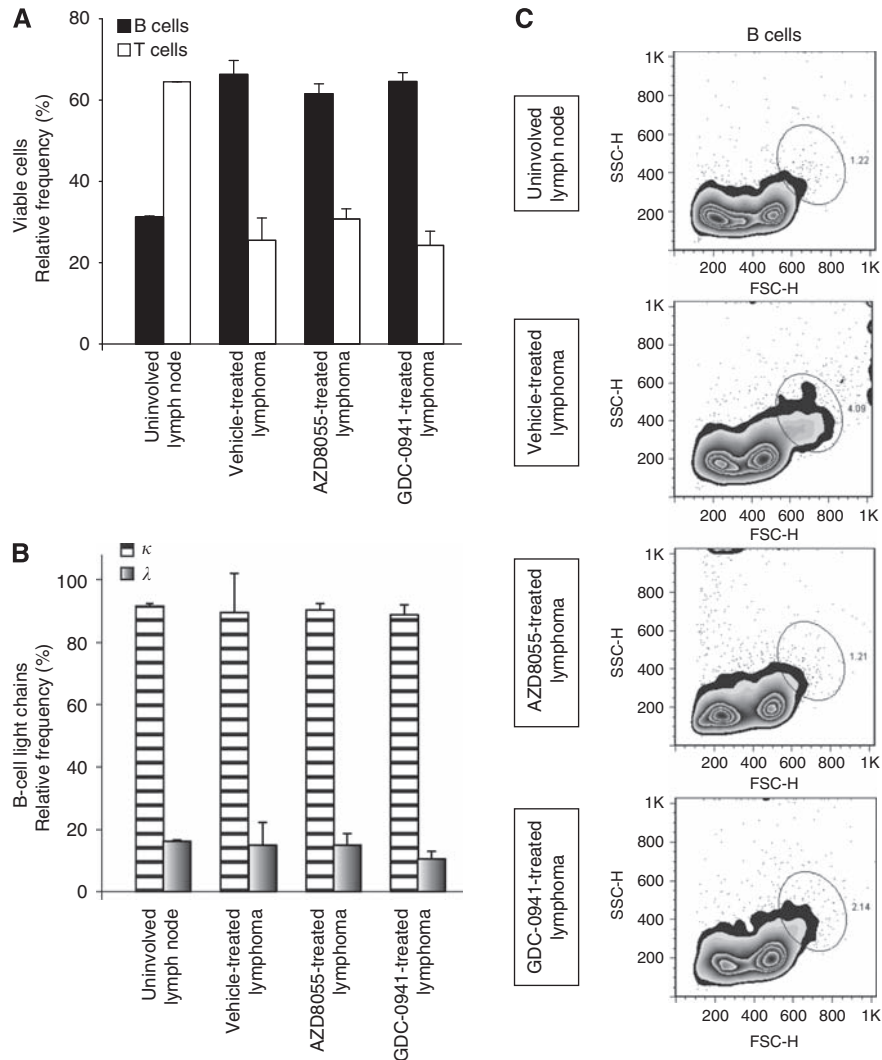
Figure 5 AZD8055 and GDC-0941 treatment impairs B-cell centroblast population. The relative frequencies of viable B and T cells (**A**) and B cells expressing κ- or λ-light chains (**B**) present in healthy uninvolved lymph nodes or tumours from mice treated as shown. Data shown are the mean of at least five tumours; error bars represent the standard error of the mean. (**C**) The forward–side scatter profiles of all (live and dead) B cells from a healthy uninvolved lymph node and tumours from mice treated as shown. Zebra plots are representative of at least five different tumours.

BJC
OPEN

PI3K and mTOR inhibitors shrink follicular lymphomas
JM García-Martínez *et al*

npg

1123

Figure 6 Post-treatment tumour growth. (**A**) As in Figure 2, mean relative tumour volumes (normalised to their size at day 0) from mice treated with either vehicle (*n* = 4), AZD8055 (20 mg kg⁻¹; *n* = 3) or GDC-0941 (75 mg kg⁻¹; *n* = 4) plotted against time. Drug treatment was ceased at day 42, and the mice were also imaged at days 63 and 77 without receiving further treatment. (**B**) Tumour volumes (normalised to their size at day 42) plotted against time. (**C** and **D**) After 35 days without treatment, tumour samples were generated and (**C**) processed for immunohistological analysis with the indicated staining, or (**D**) analysed by immunoblotting with the indicated antibodies. For each condition, immunoblots and immunostainings are representative tumour samples derived from three to four different mice.

increased Ki67 reactivity to 15–20% (Figure 6C, panels h and m), with one extreme example of high-grade Burkitt-like morphology and a Ki67 rate of >50% in one of the AZD8055-treated mouse (data not shown). There was strong cytoplasmic staining for phosphorylated ribosomal S6 protein in the now increased number of centroblasts (Figure 6C, panels i and n), with no apparent difference between the two treatment groups. The distribution of immunoreactivity for p473-Akt appeared to be unaltered by treatment, although in those later tumours of both treated and untreated groups that showed conversion to diffuse large B-cell lymphoma, Akt Ser473 phosphorylation reactivity was increased in tumour cells (Figure 6C, panels e, j and o).

Finally, we also analysed by western blot the PI3K and mTOR downstream targets within the tumour at the end of the study. Consistent with the above observations, we confirmed that the PI3K–mTOR pathway was re-activated following drug removal, and no differences were detected in high levels of phosphorylation

of endogenous NDRG1, S6K1, 4E-BP1, ribosomal S6 protein, Akt or any of its substrates analysed between control or drug-treated groups (Figure 6D).

DISCUSSION

In the present study, we have characterised the effect of oral administration of the mTOR inhibitor, AZD8055, and the PI3K inhibitor, GDC-0941, on B-cell follicular lymphoma that spontaneously develops in PTEN-deficient mice. Arguably, this model of mouse tumour is more representative of a spontaneous tumour in which the PI3K pathway is over-activated than xenograft models, frequently employed to assess effects of signal transduction inhibitors. The drugs were well tolerated, and mice administered the compounds for up to 6 weeks displayed no overt

phenotypes. The data demonstrate that the drugs effectively ablate activation of PI3K–mTOR pathway, as emphasised by the inhibition of Akt, S6K and SGK activity, and dephosphorylation of key effectors of this pathway such as 4E-BP1 within the tumour. Strikingly, AZD8055 or GDC-0941 treatment causes a marked ~40% shrinkage of tumour volume within 2 weeks, and a further ~10% reduction is observed after another 4 weeks of drug treatment. In future work, it would be interesting to evaluate whether tumours could be maintained at a reduced size for longer periods of time or whether the tumours would become resistant to the drugs and start to expand. It would also be interesting to establish whether more frequent administration of AZD8055 or GDC-0941 to maintain inhibition of the PI3K–mTOR pathways over a 24 h period would have a greater effect on reduction of tumour volume. Nevertheless, the data is encouraging, as it would indicate these compounds would offer benefit for the treatment of human cancers in which the PI3K pathway was activated.

Our data also emphasise that further work is required to identify the mechanisms by which tumours are maintained and do not regress completely despite prolonged treatment with AZD8055 or GDC-0941. More detailed analysis is required to establish whether AZD8055 or GDC-0941 exerts a cytostatic effect and stops B-cell follicular lymphoma cell proliferation rather than exerting a predominant cytotoxic effect. Several widely used anti-cancer drugs such as tamoxifen principally act by inhibiting proliferation of tumour cells rather than inducing tumour cell death (Furr and Jordan, 1984). Suppression of the PI3K and mTOR pathways also reduces cell size (Wullschleger et al, 2006). It is therefore possible that some of the regression in B-cell follicular lymphoma tumour volume observed following GDC-0941 or AZD8055 treatment is due to the effect of these drugs in diminishing cell size rather than decreasing cell number. A more in-depth analysis of tumour cell numbers and volume would be required to assess this. It is also possible that the increase in tumour growth rate after treatment results from a change to a more aggressive population of cells within the tumour. Moreover, shrinkage of the tumour could change tumour microenvironment favouring re-growth. It is also possible that prolonged treatment with GDC-0941 or AZD8055 induces resistance of tumour cells to these compounds. This could result in oligoclonal selection and could explain, in part, the more rapid disease progression observed after cessation of GDC-0941 or AZD8055 treatment (Figure 6B). In future work, it would be important to evaluate whether tumour cells did develop resistance to PI3K–mTOR pathway inhibitors and if so, work out the mechanism by which this resistance occurs. It would also be critical to investigate whether such resistance also occurs in cancer patients being treated with these compounds in clinical trials.

In addition, our data suggest that there are no major differences in the ability of GDC-0941 or AZD8055 to suppress growth or activity of Akt, S6K or SGK within B-cell follicular lymphomas. The only slight difference was that tumour re-growth following AZD8055 cessation was slightly slower than following termination of GDC-0941 administration (Figures 6A and B). PI3K pathway activates several other pathways other than the mTOR–Akt/S6K/SGK pathway including the RAC/Rho pathways that have been implicated in cancer. There are also numerous other proteins that possess PtdIns(3,4,5)P3-binding PH domains (Downes et al, 2007), which could also be implicated in regulating cell growth and proliferation downstream of PI3K. Inhibition of mTOR would not be expected to suppress these other PI3K-regulated pathways. However, the finding that PI3K and mTOR inhibitors have similar effects provides further evidence that the mTOR–Akt/S6K/SGK pathway is the most relevant axis of signalling downstream of PI3K in regulating tumour development.

Finally, our findings also emphasise that inhibition of the PI3K or mTOR pathway alone will not be sufficient to cause complete regression of such tumours. Interestingly, different studies have shown that treatment of follicular lymphoma cell lines with combinations of PI3K/Akt/mTOR pathway inhibitors and the proteosome inhibitor Bortezomib, or the anti-apoptotic Bcl-2 family members inhibitor ABT-263, synergise to inhibit cell proliferation and promote apoptosis (Ackler et al, 2008; Bhende et al, 2010). In future work, it would be interesting to analyse the effects that combining these inhibitors with AZD8055 or GDC-0941 have on treatment of B-cell follicular lymphoma. It would also be interesting to extend this analysis to other tumours in mice models employing inhibitors of other components of the PI3K pathway, such as Akt, PDK1, S6K1 and SGK isoforms, that are becoming available. As there is also considerable emerging evidence that dual inhibition of the PI3K and ERK pathways is more effective at inhibiting tumourigenesis than inhibition of either pathway alone (She et al, 2005; Carracedo et al, 2008; Engelman et al, 2008), it may therefore be necessary to combine these inhibitors with an inhibitor of the ERK pathway.

In summary, we have shown that studying the effect of new drugs with a combination of MRI analysis and specific types of spontaneously preformed tumours is capable of producing strong preclinical data about the effectiveness of new drugs in specific types of cancer. Our data suggest that AZD8055 and GDC-0941 treatment would offer benefit for the treatment of cancers in which the PI3K pathway is inappropriately activated; however, new combination strategies would need to be tested to induce the complete regression of such tumours. We propose that the spontaneous cancer model elaborated in our study could be utilised to benchmark the relative effectiveness of PI3K/mTOR inhibitors at suppressing tumour growth.

REFERENCES

Ackler S, Xiao Y, Mitten MJ, Foster K, Oleksijew A, Refici M, Schlessinger S, Wang B, Chemburkar SR, Bauch J, Tse C, Frost DJ, Fesik SW, Rosenberg SH, Elmore SW, Shoemaker AR (2008) ABT-263 and rapamycin act cooperatively to kill lymphoma cells *in vitro* and *in vivo*. *Mol Cancer Ther* 7: 3265–3274

Bayascas JR, Leslie NR, Parsons R, Fleming S, Alessi DR (2005) Hypomorphic mutation of PDK1 suppresses tumorigenesis in PTEN (+/−) mice. *Curr Biol* 15: 1839–1846

Bhende PM, Park SI, Lim MS, Dittmer DP, Damania B (2010) The dual PI3K/mTOR inhibitor, NVP-BEZ235, is efficacious against follicular lymphoma. *Leukemia* 24(10): 1781–1784

Carracedo A, Ma L, Teruya-Feldstein J, Rojo F, Salmena L, Alimonti A, Egia A, Sasaki AT, Thomas G, Kozma SC, Papa A, Nardella C, Cantley LC, Baselga J, Pandolfi PP (2008) Inhibition of mTORC1 leads to MAPK pathway activation through a PI3K-dependent feedback loop in human cancer. *J Clin Invest* 118: 3065–3074

Chen ML, Xu PZ, Peng XD, Chen WS, Guzman G, Yang X, Di Cristofano A, Pandolfi PP, Hay N (2006) The deficiency of Akt1 is sufficient to suppress tumor development in Pten+/− mice. *Genes Dev* **20:** 1569 – 1574

Chresta CM, Davies BR, Hickson I, Harding T, Cosulich S, Critchlow SE, Vincent JP, Ellston R, Jones D, Sini P, James D, Howard Z, Dudley P, Hughes G, Smith L, Maguire S, Hummersone M, Malagu K, Menear K, Jenkins R, Jacobsen M, Smith GC, Guichard S, Pass M (2010) AZD8055 is a potent, selective, and orally bioavailable ATP-competitive mammalian target of rapamycin kinase inhibitor with *in vitro* and *in vivo* antitumor activity. *Cancer Res* **70:** 288 – 298

Collins BJ, Deak M, Murray-Tait V, Storey KG, Alessi DR (2005) *In vivo* role of the phosphate groove of PDK1 defined by knockin mutation. *J Cell Sci* **118:** 5023 – 5034

Di Cristofano A, Pesce B, Cordon-Cardo C, Pandolfi PP (1998) Pten is essential for embryonic development and tumour suppression. *Nat Genet* **19:** 348 – 355

Downes CP, Leslie NR, Batty IH, van der Kaay J (2007) Metabolic switching of PI3K-dependent lipid signals. *Biochem Soc Trans* **35:** 188 – 192

Engelman JA (2009) Targeting PI3K signalling in cancer: opportunities, challenges and limitations. *Nat Rev Cancer* **9:** 550 – 562

Engelman JA, Chen L, Tan X, Crosby K, Guimaraes AR, Upadhyay R, Maira M, McNamara K, Perera SA, Song Y, Chirieac LR, Kaur R, Lightbown A, Simendinger J, Li T, Padera RF, Garcia-Echeverria C, Weissleder R, Mahmood U, Cantley LC, Wong KK (2008) Effective use of PI3K and MEK inhibitors to treat mutant Kras G12D and PIK3CA H1047R murine lung cancers. *Nat Med* **14:** 1351 – 1356

Engelman JA, Luo J, Cantley LC (2006) The evolution of phosphatidylinositol 3-kinases as regulators of growth and metabolism. *Nat Rev Genet* **7:** 606 – 619

Folkes AJ, Ahmadi K, Alderton WK, Alix S, Baker SJ, Box G, Chuckowree IS, Clarke PA, Depledge P, Eccles SA, Friedman LS, Hayes A, Hancox TC, Kugendradas A, Lensun L, Moore P, Olivero AG, Pang J, Patel S, Pergl-Wilson GH, Raynaud FI, Robson A, Saghir N, Salphati L, Sohal S, Ultsch MH, Valenti M, Wallweber HJ, Wan NC, Wiesmann C, Workman P, Zhyvoloup A, Zvelebil MJ, Shuttleworth SJ (2008) The identification of 2-(1H-indazol-4-yl)-6-(4-methanesulfonyl-piperazin-1-ylmethyl)-4-morpholin -4-yl-thieno[3,2-d]pyrimidine (GDC-0941) as a potent, selective, orally bioavailable inhibitor of class I PI3 kinase for the treatment of cancer. *J Med Chem* **51:** 5522 – 5532

Furr BJ, Jordan VC (1984) The pharmacology and clinical uses of tamoxifen. *Pharmacol Ther* **25:** 127 – 205

Garcia-Martinez JM, Alessi DR (2008) mTOR complex 2 (mTORC2) controls hydrophobic motif phosphorylation and activation of serum- and glucocorticoid-induced protein kinase 1 (SGK1). *Biochem J* **416:** 375 – 385

Guertin DA, Stevens DM, Saitoh M, Kinkel S, Crosby K, Sheen JH, Mullholland DJ, Magnuson MA, Wu H, Sabatini DM (2009) mTOR complex 2 is required for the development of prostate cancer induced by Pten loss in mice. *Cancer Cell* **15:** 148 – 159

Haas-Kogan D, Shalev N, Wong M, Mills G, Yount G, Stokoe D (1998) Protein kinase B (PKB/Akt) activity is elevated in glioblastoma cells due to mutation of the tumor suppressor PTEN/MMAC. *Curr Biol* **8:** 1195 – 1198

Harris NL, Jaffe ES, Diebold J, Flandrin G, Muller-Hermelink HK, Vardiman J, Lister TA, Bloomfield CD (1999) The World Health Organization classification of neoplastic diseases of the hematopoietic and lymphoid tissues. Report of the Clinical Advisory Committee meeting, Airlie House, Virginia, November, 1997. *Ann Oncol* **10:** 1419 – 1432

Huang X, Wullschleger S, Shpiro N, McGuire VA, Sakamoto K, Woods YL, McBurnie W, Fleming S, Alessi DR (2008) Important role of the LKB1-AMPK pathway in suppressing tumorigenesis in PTEN-deficient mice. *Biochem J* **412:** 211 – 221

Leslie NR, Downes CP (2004) PTEN function: how normal cells control it and tumour cells lose it. *Biochem J* **382:** 1 – 11

Maehama T, Dixon JE (1998) The tumor suppressor, PTEN/MMAC1, dephosphorylates the lipid second messenger, phosphatidylinositol 3,4,5-trisphosphate. *J Biol Chem* **273:** 13375 – 13378

Murray JT, Campbell DG, Morrice N, Auld GC, Shpiro N, Marquez R, Peggie M, Bain J, Bloomberg GB, Grahammer F, Lang F, Wulff P, Kuhl D, Cohen P (2004) Exploitation of KESTREL to identify NDRG family members as physiological substrates for SGK1 and GSK3. *Biochem J* **384:** 477 – 488

Myers MP, Pass I, Batty IH, Van der Kaay J, Stolarov JP, Hemmings BA, Wigler MH, Downes CP, Tonks NK (1998) The lipid phosphatase activity of PTEN is critical for its tumor supressor function. *Proc Natl Acad Sci USA* **95:** 13513 – 13518

Pearce LR, Komander D, Alessi DR (2010) The nuts and bolts of AGC protein kinases. *Nat Rev Mol Cell Biol* **11:** 9 – 22

Podsypanina K, Ellenson LH, Nemes A, Gu J, Tamura M, Yamada KM, Cordon-Cardo C, Catoretti G, Fisher PE, Parsons R (1999) Mutation of Pten/Mmac1 in mice causes neoplasia in multiple organ systems. *Proc Natl Acad Sci USA* **96:** 1563 – 1568

Sakamoto K, McCarthy A, Smith D, Green KA, Grahame Hardie D, Ashworth A, Alessi DR (2005) Deficiency of LKB1 in skeletal muscle prevents AMPK activation and glucose uptake during contraction. *EMBO J* **24:** 1810 – 1820

Salphati L, Wong H, Belvin M, Bradford D, Edgar KA, Prior WW, Sampath D, Wallin JJ (2010) Pharmacokinetic-pharmacodynamic modeling of tumor growth inhibition and biomarker modulation by the novel phosphatidylinositol 3-kinase inhibitor GDC-0941. *Drug Metab Dispos* **38:** 1436 – 1442

Samuels Y, Wang Z, Bardelli A, Silliman N, Ptak J, Szabo S, Yan H, Gazdar A, Powell SM, Riggins GJ, Willson JK, Markowitz S, Kinzler KW, Vogelstein B, Velculescu VE (2004) High frequency of mutations of the *PIK3CA* gene in human cancers. *Science* **304:** 554

She QB, Solit DB, Ye Q, O'Reilly KE, Lobo J, Rosen N (2005) The BAD protein integrates survival signaling by EGFR/MAPK and PI3K/Akt kinase pathways in PTEN-deficient tumor cells. *Cancer Cell* **8:** 287 – 297

Stambolic V, Suzuki A, de la Pompa JL, Brothers GM, Mirtsos C, Sasaki T, Ruland J, Penninger JM, Siderovski DP, Mak TW (1998) Negative regulation of PKB/Akt-dependent cell survival by the tumor suppressor PTEN. *Cell* **95:** 29 – 39

Sulis ML, Parsons R (2003) PTEN: from pathology to biology. *Trends Cell Biol* **13:** 478 – 483

Suzuki A, de la Pompa JL, Stambolic V, Elia AJ, Sasaki T, del Barco Barrantes I, Ho A, Wakeham A, Itie A, Khoo W, Fukumoto M, Mak TW (1998) High cancer susceptibility and embryonic lethality associated with mutation of the *PTEN* tumor suppressor gene in mice. *Curr Biol* **8:** 1169 – 1178

Taddesse-Heath L, Morse HC (2000) Lymphoma in genetically engineered mice. In *Pathology of genetically engineered mice*, Ward JM, Mahler JF, Maronpot RR, Sundberg JP (eds). 1st edition, Chapter 24. pp 365 – 382. Ames: Iowa State University Press

Thoreen CC, Kang SA, Chang JW, Liu Q, Zhang J, Gao Y, Reichling LJ, Sim T, Sabatini DM, Gray NS (2009) An ATP-competitive mammalian target of rapamycin inhibitor reveals rapamycin-resistant functions of mTORC1. *J Biol Chem* **284:** 8023 – 8032

Wullschleger S, Loewith R, Hall MN (2006) TOR signaling in growth and metabolism. *Cell* **124:** 471 – 484

Wullschleger S, Sakamoto K, Johnstone L, Duce S, Fleming S, Alessi DR (2010) How moderate changes in Akt T-loop phosphorylation impact on tumorigenesis and insulin resistance. *Dis Model Mech Oct* **4**(1): 95 – 103

Translational Therapeutics